# Potential-induced acid-base chemistry of adsorbed species

Harlan Mantelli [a], Ricardo Martinez-Hincapie [b], Juan Feliu [b], Daniel Scherson [a, *]

[a] Department of Chemistry, Case Western Reserve University, Cleveland, OH, USA
[b] Instituto de Electroquímica, Universidad de Alicante, Alicante, Spain

## ARTICLE INFO

## ABSTRACT

The $pK_a$ of bicarbonate ion adsorbed on the surface of Pt(111), $HCO_3^-(ads)$, in $CO_2$-saturated $KClO_4/HClO_4$ aqueous solutions has been determined by judicious application of a theoretical model originally proposed by Smith and White (*Langmuir* **1993**, *9* (1), 1−3) to explain voltammetric features found for non-redox active alkyl chain monolayers bearing carboxylic moieties irreversibly bound to gold surfaces. The analysis herein presented relied on $HCO_3^-(ads)$ and $CO_3^{2-}(ads)$ coverages derived from in situ Fourier transform infrared spectroscopy measurements as a function of potential and $pH$ reported by Martinez-Hincapie et al. (*J. Phys. Chem. C* **2016**, *120* (29), 16191−16199), as input parameters, yielding a $pK_a$ for $HCO_3^-(ads)$ of ca. $2.6 \pm 0.2$. This value is significantly smaller than that of $HCO_3^-(aq)$ in bulk solutions, a phenomenon associated with the bonding of the species to the electrode surface, a factor that markedly modifies its acid base characteristics.

© 2019 Published by Elsevier Ltd.

## 1. Introduction

In a recent paper, Martinez-Hincapie et al. [1] reported in situ reflection-absorption Fourier transform infrared spectra for a Pt(111) electrode in $CO_2$-saturated $KClO_4/HClO_4$ aqueous solutions of $pH$ values ranging from 0.38 to 3.10 as a function of the applied potential, E. Quantitative analyses of the data collected revealed significant changes in the relative ratios of the integrated intensities of the peaks, and thus in the coverage of adsorbed bicarbonate, $HCO_3^-(ads)$, and carbonate, $CO_3^{2-}(ads)$, with both E and $pH$. Shown in scattered symbols in Fig. 1 are plots of $\log\left[\Gamma_{CO_3^{2-}}/\Gamma_{HCO_3^-}\right]$ vs E, where $\Gamma_{CO_3^{2-}}$ and $\Gamma_{HCO_3^-}$, are the surface concentrations of $HCO_3^-(ads)$ and $CO_3^{2-}(ads)$, respectively, for solutions of six different $pH$ reported in the cited reference, where the solid lines are linear fits to the data. This procedure made it possible to determine potential values for which $\log\left[\Gamma_{CO_3^{2-}}(ads)/\Gamma_{HCO_3^-}\right] = 0$, i.e. the intersections of the solid lines with the x-axis line in Fig. 1, for each of the solutions, which they then used to construct a plot of $pH$@ $\log\left[\Gamma_{CO_3^{2-}}/\Gamma_{HCO_3^-}\right] = 0$ vs E (see Fig. S1). A linear fit to the resulting data (see line in Fig. S1 yielded, upon interpolation, a value of ca. 5 at the potential of zero free charge (pzfc), which they defined as

the $pK_a$ of $HCO_3^-(ads)$ under the conditions in which the experiments were performed. It should be emphasized that the procedure employed for determining this latter parameter is based on a simple analysis of band intensities and mass balance, and, as such, does not rely on any specific interfacial model.

The presence of these highly ionized adsorbed species in solutions of such low $pH$, as well as the changes in the extent of ionization induced by the applied potential, represent a new phenomenon not as yet fully understood.

This communication will show that these effects can be accounted for by judicious application of a model reported by Smith and White [2] decades ago, aimed at explaining the presence of voltammetric peaks for mixed 11-mercaptoundecanoic acid and 1-decanethiol layers self-assembled on Ag(111) in aqueous electrolytes [3]. Additional experimental evidence in support of this model was reported by Bryant and Crooks [4] for 4-mercaptopyridine and 4-aminothiophenol monolayers adsorbed on polycrystalline Au in similar solutions. It may be noted that Fawcett et al. further refined this theory by introducing discreteness of charge effects [5,6]. However, these factors will not be considered in our analysis. As will be shown, the original model, can correctly predict the potential dependence of the relative ratios of $\Gamma_{CO_3^{2-}}$ and $\Gamma_{HCO_3^-}$ in the adsorbed layer on Pt(111) as a function of $pH$, assuming reasonable values for the parameters involved. Particularly striking was the much lower $pK_a$ for $HCO_3^-(ads)$ determined from this analysis compared to that in bulk aqueous solutions, a phenomenon we

---

* Corresponding author.
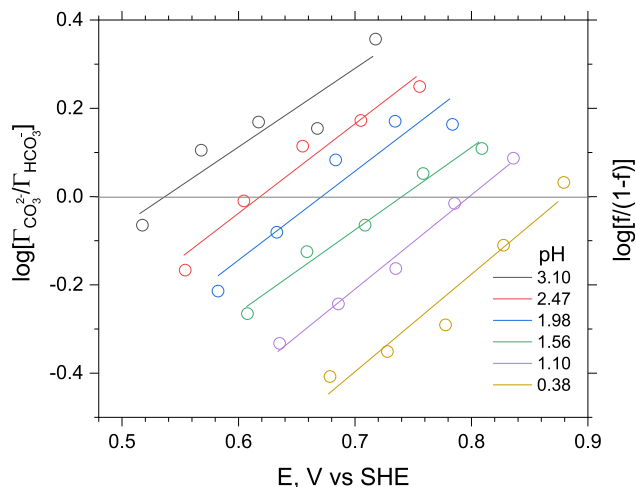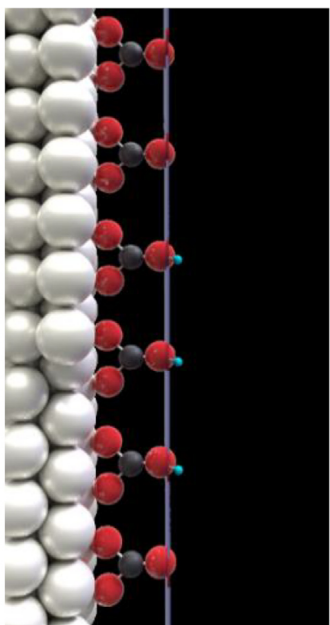  E-mail address: dxs16@case.edu (D. Scherson).

**Fig. 1.** Plots of $\log\left[\Gamma_{CO_3^{2-}}/\Gamma_{HCO_3^-}\right]$ $(=\log[f/(1-f)])$ vs E extracted from the spectroscopic data (scattered symbols), where the solid lines are linear fits to the data collected at the specific $pH$ as reported by Martinez-Hincapie et al. [1].

tentatively ascribe to the bonding of the adsorbate to the surface and thus to changes in its electronic structure.

## 2. Theoretical aspects

The starting point of our analysis regards the two species in the $HCO_3^-(ads)/CO_3^{2-}(ads)$ layer, as attached to the surface through a bidentate-type bond with the proton in $HCO_3^-(ads)$ bonded to the oxygen facing the electrolyte, which, within the Smith and White [2] model, defines the so-called plane of acid dissociation (PAD)



**Fig. 2.** Schematic diagram of $HCO_3^-(ads)/CO_3^{2-}(ads)$ layer on a metal electrode, where M, PAD and S define, respectively, the metal, the plane of acid dissociation and the electrolyte solution.

(see Fig. 2). Based on their formalism, the problem so stated reduces to finding solutions of a system of five non-linear algebraic equations with five unknowns i.e. $\sigma_M$, $\sigma_{PAD}$, $\Delta V_F$, $\Delta V_S$ and $pK_a$.

$$\sigma_M = C_F \Delta V_F \tag{1}$$

$$E - E_{pzc} = \Delta V_F + \Delta V_S \tag{2}$$

$$\sigma_M + \sigma_{PAD} = \varepsilon_0 \varepsilon_S \kappa \frac{2kT}{e} \sinh\left\{\frac{e\Delta V_S}{2kT}\right\} \tag{3}$$

$$\log\left[\frac{f}{1-f}\right] = pH - pK_a + \frac{e\Delta V_S}{2.3kT} \tag{4}$$

$$\sigma_{PAD} = -\Gamma_T F f \tag{5}$$

where $\sigma_M$ and $\sigma_{PAD}$ are the charge densities on the electrode and at the PAD ($\mu C/cm^2$), respectively, $\Delta V_F = \phi_M - \phi_{PAD}$ and $\Delta V_S = \phi_{PAD} - \phi_S$, where the $\phi_i$'s are the electrostatic potentials at the metal, the PAD, and in the electrolyte solution, S, respectively (see Fig. 2). $pK_a$ is the acidity constant of $HCO_3^-(ads)$. Furthermore, the symbol $C_F$ in Eq. (1) is the capacitance of the adsorbed molecular film ($\mu F/cm^2$), $E$ represents the potential at which each of the measurements was collected and $E_{pcz}$ in Eq. (2) is the potential of zero charge of the interface devoid of the adsorbates, (V), and $\Gamma_T$ in Eq. (5) is the **saturation** coverage of the adsorbed species regardless of its extent of protonation (mol/cm$^2$). Eq. (3) represents the neutral character of the interface, where its right hand side is the charge density of the diffuse double layer, $\sigma_S$, ($\mu C/cm^2$), written in terms of $\Delta V_s$, the reciprocal Debye length, $\kappa$, the dielectric constants of vacuum, $\varepsilon_0$, and the electrolyte solution, $\varepsilon_s$. Lastly, $f$ is defined as $\Gamma_{CO_3^{2-}}/\left[\Gamma_{CO_3^{2-}} + \Gamma_{HCO_3^-}\right]$, i.e. the fraction of adsorbed species in the deprotonated state; hence, $\log\left[\Gamma_{CO_3^{2-}}/\Gamma_{HCO_3^-}\right] = f/(1-f)$ and other quantities have their usual meaning (see Table 1). It is important to note that some of the data at lower potentials collected by Martinez-Hincapie et al. led to values of $\Gamma_{CO_3^{2-}} + \Gamma_{HCO_3^-} < \Gamma_T$, and, as such, were excluded from this analysis.

The system of Eq. (1) through (5) was solved using Mathematica 11.3 using each of the $f$ values extracted from the analysis of the spectroelectrochemical measurements at the specified $E$ and $pH$ for which the potential was high enough for the monolayer to achieve its saturation value. Approximate values of the parameters involved, i.e. $C_F$, $\Gamma_T$, $\kappa$ and $E_{pzc}$. were obtained from literature data. In

**Table 1**
Symbols, definitions and magnitudes of the optimized parameters involved in the model.

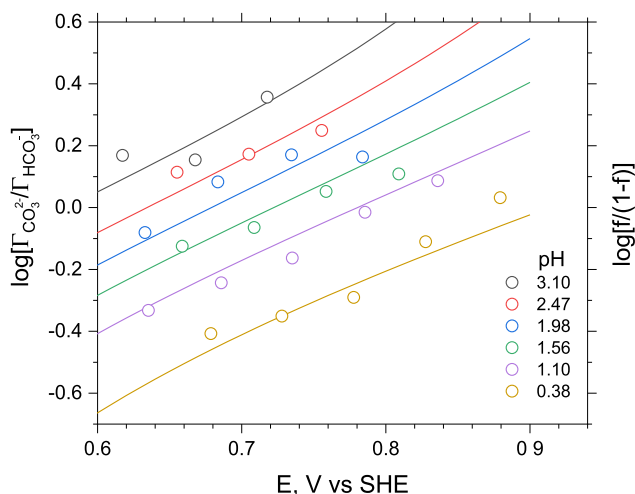| Symbol | Name | Value |
|---|---|---|
| T | Temperature | 293 K |
| Epzc | Potential of Zero Charge (pzc) of Pt (111) | 0.33 V vs SHE |
| $\varepsilon_0$ | Permittivity of Vacuum | $8.85 \times 10^{-8}$ μF/cm |
| $\varepsilon_S$ | Dielectric Constant of Water | 78 |
| $\kappa$ | Reciprocal Debye length in 0.1 M aqueous electrolyte at 293 K | $1.052 \times 10^7$ cm$^{-1}$ |
| $c_0$ | Electrolyte Concentration | $10^{-4}$ mol/cm$^3$ |
| $\Gamma_T$ | Saturation Surface Coverage of Adsorbate | $8.5 \times 10^{-10}$ mol/cm$^2$ |
| $C_F$ | Film Capacitance | 140 μF/cm$^2$ |
| e | Elementary Charge | $1.602 \times 10^{-13}$ μC |
| F | Faraday's Constant | $9.6485 \times 10^{11}$ μC/mol |
| k | Boltzmann's Constant | $1.38 \times 10^{-19}$ cm$^2\cdot$kg$\cdot$s$^{-2}\cdot$K$^{-1}$ |
| R | Gas Constant | $8.31 \times 10^4$ cm$^2\cdot$kg$\cdot$s$^{-2}\cdot$K$^{-1}\cdot$mol$^{-1}$ |

**Fig. 3.** Plots of $\log\left[\Gamma_{CO_3^{2-}}/\Gamma_{HCO_3^-}\right]$ $(= \log[f/(1-f)])$ vs E extracted from the spectroscopic data (scattered symbols) reported by Martinez-Hincapie et al. [1] The solid lines were obtained from the application of the Smith and White model [2] for optimized values of the parameters involved. i.e. $E_{pzc} = 0.33$ V vs SHE, $C_F = 140$ $\mu$C/cm², $\Gamma_T = 8.5 \times 10^{-10}$ mol/cm² (see text for details) assuming $pK_a = 2.6$, the rounded average of the entire set of data (see text for details).

particular, $C_F$ was obtained from the voltammetric curves at potentials positive to the rather broad peak centered at ca. 0.65 V (see Fig. 1 in Ref. 1), $\Gamma_T$ was selected within the range of saturation coverages of the $HCO_3^-(ads)/CO_3^{2-}(ads)$ layer reported by Iwasita et al. [7], i.e. $6.6-8.3 \times 10^{-10}$ mol/cm², and $E_{pzc}$ was taken from a reported value of ca. 0.3 V vs SHE [8]. Lastly, the reciprocal Debye length, $\kappa$, was calculated based on the 0.1 M electrolyte concentration used in the experiments (see Table 1). Initial attempts to obtain numerical solutions failed to converge, a problem that was traced to the simultaneous use of two non-linear functions as

provided by Mathematica, log(x) and sinh(x). These difficulties could be overcome by approximating the latter by a 5th degree Taylor expansion, which reproduced the analytical function within 0.1% percent (see Fig. S2 in the Supplementary Material). Shown in Fig. S3 in the Supplementary Material, as means of illustration, are plots of $\sigma_M$ (Panel A), $\sigma_{PAD}$ (B), $\Delta V_F$ (C), $\Delta V_S$ (D), and $pK_a$ (E), as a function of the rational potential, i.e. $E - E_{pzc}$, for the six solutions with different $pH$ values reported in Ref. 1, assuming $\Gamma_T = 7.5 \times 10^{-10}$ mol/cm², $C_F = 150$ $\mu$F/cm², and $E_{pzc} = 0.3$ V vs SHE. The solid lines in Fig. S4 were calculated by solving the system of equations for $f$, and setting $pK_a = 3.2$, which corresponds to the average value determined from the entire set of data collected for this specific set of parameters.

While the overall trends do track the experimental data, the quantitative agreement is rather poor. As shown in Fig. 3, significant improvement was achieved by setting $\Gamma_T = 8.5 \times 10^{-10}$ mol/cm², $C_F = 140$ $\mu$F/cm² and $E_{pzc} = 0.33$ V vs SHE, which are still within the expected uncertainty ranges, while keeping the rest of the parameters fixed (see Table 1).

The corresponding plots of $\sigma_M$ (Panel A), $\sigma_{PAD}$ (B), $\Delta V_F$ (C), $\Delta V_S$ (D), and $pK_a$ (E), as a function of E in this case, are shown in Fig. 4. In particular, the spread of $pK_a$ values (see Panel E, Fig. 4) was reduced to less than ca. one unit, and the fit of the predicted to the experimental data in Fig. 3 (see solid lines) was vastly improved.

Further support for this proposed model was obtained from the normal probability plot of the entire set of $pK_a$ values shown in Fig. 5, where the red line represents a normal distribution and the black lines embrace a 95% confidence interval, which yielded a mean of 2.6 and a standard deviation of 0.2. Moreover, evidence that the $pK_a$ value is indeed unique, as prescribed by the Smith and White model, was obtained from the analysis of the dependence of $pK_a$ on $pH$ and also on E. As shown in the Supplementary Material (see Fig. S5), the ANOVA test yielded, for the first case, a value of $p = 0.95$, and an adjusted $R^2 = 0.001$, suggesting that it is extremely unlikely that the data is represented by a linear fit. The same conclusions were drawn from the analysis of the $pH$ values as a
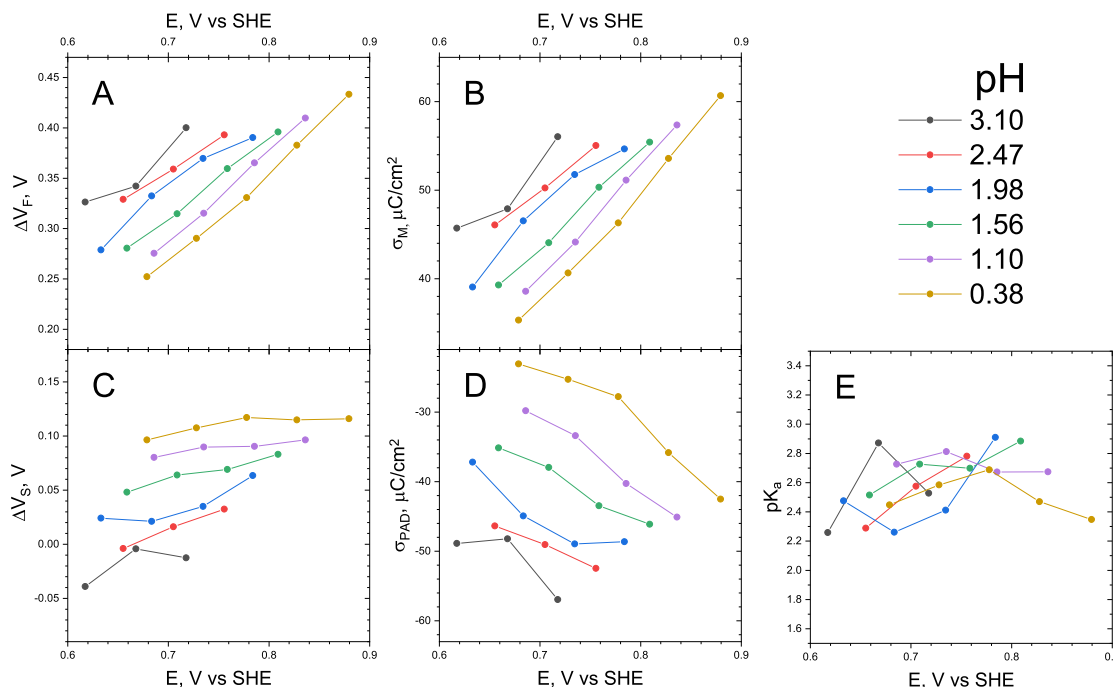


**Fig. 4.** Plots of $\Delta V_F$ (Panel A), $\sigma_M$ (B), $\Delta V_S$ (C), $\sigma_{PAD}$ (D) and $pK_a$ (E) as a function of potential based on the model herein proposed. The parameters used in the simulation are listed in Table 1.
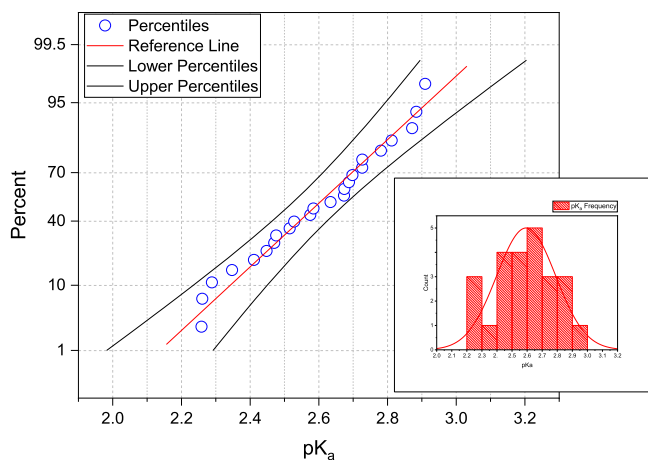
**Fig. 5.** Normal probability plot of the entire set of $pK_a$ values. The red line represents a normal distribution and the black lines embrace a 95% confidence interval. This analysis yielded a mean of 2.6 and a standard deviation of 0.2. Insert: Histogram of the $pK_a$ data. (For interpretation of the references to colour in this figure legend, the reader is referred to the Web version of this article.)

function of E (see Fig. S6), for which the ANOVA test yielded p = 0.41, and $R^2 = 0.03$, meaning that the slope of the linear fit is not significantly different from 0, and that a linear fit is also not representative of the data.

In conclusion, application of the Smith and White model to the $HCO_3^- (ads) / CO_3^{2-} (ads)$ layer on Pt(111) can successfully account for the changes in the extent of dissociation of $HCO_3^- (ads)$ with potential and solution $pH$, as determined from the analysis of in situ Fourier transform infrared spectra. As evidenced from the results obtained, the $pK_a$ of $HCO_3^- (ads) = 2.6 \pm 0.2$, is significantly shifted toward lower values compared to that of the same species in bulk solution. Interestingly, this effect is opposite to that found for alkyl thiol monolayers bearing carboxylic groups at the terminus facing the aqueous electrolyte, in which case the $pK_a$ of the monolayer was found to shift up over three units compared to, for example, acetic acid [9]. Extensions of this approach to the adsorption of other acid-base ions, such as phosphate, are now being considered, and will be reported in due course.

## Acknowledgements

## Appendix A. Supplementary data

Supplementary data to this article can be found online at https://doi.org/10.1016/j.electacta.2019.134793.

## References

[1] R. Martinez-Hincapie, A. Berna, A. Rodes, V. Climent, J.M. Feliu, Surface acid-base properties of anion-adsorbed species at Pt(111) electrode surfaces in contact with CO2-containing perchloric acid solutions, J. Phys. Chem. C 120 (29) (2016) 16191–16199.
[2] C.P. Smith, H.S. White, Voltammetry of molecular films containing acid-base groups, Langmuir 9 (1) (1993) 1–3.
[3] H.S. White, J.D. Peterson, Q.Z. Cui, K.J. Stevenson, Voltammetric measurement of interfacial acid/base reactions, J. Phys. Chem. B 102 (16) (1998) 2930–2934.
[4] M.A. Bryant, R.M. Crooks, Determination of surface $pK_a$ values of surface-confined molecules derivatized with $pH$-sensitive pendant groups, Langmuir 9 (2) (1993) 385–387.
[5] R. Andreu, W.R. Fawcett, Discreteness-of-Charge effects at molecular films containing acid/base groups, J. Phys. Chem. 98 (48) (1994) 12753–12758.
[6] W.R. Fawcett, M. Fedurco, Z. Kovacova, Double-layer effects at molecular films containing acid-base groups, Langmuir 10 (7) (1994) 2403–2408.
[7] T. Iwasita, A. Rodes, E. Pastor, Vibrational spectroscopy of carbonate adsorbed on Pt(111) and Pt(110) single-crystal electrodes, J. Electroanal. Chem. 383 (1–2) (1995) 181–189.
[8] V. Climent, N. García-Araez, E. Herrero, J. Feliu, Potential of zero total charge of platinum single crystals: a local approach to stepped surfaces vicinal to Pt(111), Russ. J. Electrochem. 42 (11) (2006).
[9] S.S. Cheng, D.A. Scherson, C.N. Sukenik, In situ observation of monolayer self-assembly by FTIR/ATR, J. Am. Chem. Soc. 114 (13) (1992) 5436–5437.

## List of Symbols

$\sigma_M$: charge density on the electrode, $C/cm^2$
$\sigma_{PAD}$: charge density at the PAD, $C/cm^2$
$\sigma_S$: charge density of the diffuse double layer, $C/cm^2$
$f$: fractional surface coverage of $HCO_3^- (ads)$ at the PAD
$\Delta V_F$: potential drop across the electrode and the PAD, V
$\Delta V_S$: potential drop across the PAD and the bulk solution, V
$E$: applied voltage, V
$\Gamma_T$: saturation coverage of the $HCO_3^- (ads) / CO_3^{2-} (ads)$ layer, $mol/cm^2$